Supporting Information

Self-assembly promoted stratified multifunctional hybrid coating with self-healing ability for superior adhesion strength and hardness

*Diksha Sharma and Debaprasad Mandal**

Department of Chemistry, Indian Institute of Technology Ropar, Punjab 140001, India

E-mail: dmandal@iitrpr.ac.in

Experimental

Materials. Tannic acid (HPLC, 90%), Tetraethoxysilane (TEOS) (Alfa Aesar, 98%); Poly(vinyl alcohol) (M_w 85,000-1,24000, 99+% hydrolyzed, sigma-Aldrich), *n*-valeraldehyde (VD) (Spectrochem, 98%) were used as received.

Film formation

Polymer films were casted using bar coating method with a film applicator setting of 250 µm and allowed 2 h to ensure equilibrium followed by solvent evaporation at room temperature. Traces of solvent were eliminated by drying the polymeric film at 70 °C for 1 h. All the films were casted following a similar procedure having a thickness between 160-170 µm. Water contact angle (WCA) was measured after film formation to ensure equilibrium in the films.

Characterization methods

NMR and FT-IR

NMR spectra were collected using a JEOL JNM-ECS 400 spectrometer at ambient probe temperatures and are referenced as follows: ^{29}Si. FT-IR spectra were acquired with ATR on a BRUKER TENSOR-27 spectrometer in the range of 500 to 4000 cm^{-1} (spectral resolution = 4 cm^{-1}; 100 scans).

Thermal analysis

Thermogravimetric analysis (TGA) was performed under nitrogen atmosphere on a "TGA/DSC 1" instrument with an SDTA sensor from Mettler Toledo and data were analyzed with STARe software (version 12.1). The temperature, weight, and tau lag were calibrated using an aluminium/zinc standard sample. High-purity nitrogen (99.999%) was passed at a flow rate of 50 mL/min throughout the experiments to avoid contamination from the external atmosphere. The experiments were performed using an alumina pan as the sample holder and as the

reference using 5 to 20 mg samples. Thermal stability was investigated by heating from 30 °C to 800 °C at a heating rate of 10 °C min^{-1}. Each sample was tested at least thrice with an error limit of <2%.

UV-vis spectroscopy

The transmittance of the film coated on the glass slide was analyzed by the solid-state UV-2600 spectrophotometer SHIMADZU. To determine the transmittance of the coated material, we used quartz glass as a reference, which has 100% transmittance, and the transmittance of the other coated material in comparison to the quartz glass.

Microscope camera

The optical images of the cut sample and recovery of the crosslinked polymer were analyzed using OLYMPUS equipment (V-TV0.5XC-3, T7).

Self-Healing Test

The healing efficiency was calculated as the ratio of the mechanical performance (elongation upon break) of the repaired sample to that of the original sample using the following equation:

$$\textit{Self-healing efficiency} = \frac{performance\ of\ the\ self-healed\ sample}{performane\ of\ the\ original\ sample} \times 100$$

Water contact angle (WCA).

A sessile syringe was used to deposit water drops on polymeric films. The sessile water drop method was used to measure contact angles by Kyowa contact angles meters DMe-211 plus. The average WCA (H_2O) value was taken from five samples of the same polymer in 2.0 μL volume using a 0.305 mm wide needle, and the solvent contact angle (SCA) was determined using hexadecane in a 2.0 μL volume. The surface energy is obtained directly from the instrument applying the **Kaelble-Uy equation**.

Tensile testing

Tensile tests were performed on a Tinius Olsen H50KS instrument equipped with serrated calipers at a closure pressure of 10 psi and a strain speed of 0.3 mm min^{-1}. Rectangular (40.86 mm, 8.56 mm) thin films of **P2** and **P5** polymer samples were measured with a calliper and tensile test before and after the healing tests. For each sample, all measurements were performed at least three times.

Adhesion property

The adhesion strength of the polymeric material P5 coated on glass, aluminium, and PMMA sheet was studied by peeling test using Zwick Roell universal tensile testing machine. The surfaces of the substrates, like glass, aluminium, and PMMA were washed with acetone. The material peeled off from substrates at different adhesion strengths analysed by UTM. The specimens were extended at 0.5 mm/min at room temperature. All measurement was repeated at least 3 times for each sample.

SEM

SEM analysis was conducted on the film specimen using a JEOL JSM-6610 LA (Jeol, Japan). Integrated JEOL Analysis Station software was used for data collection and analysis. The coated sample itself was fixed onto an aluminium stage, ensuring the carbon-coated surface was in good contact with the holder. Polymer films were covered with thin platinum film.

FESEM-EDX analysis

FESEM analysis was conducted on the powder specimen using a JEOL 7610FPLUS (Jeol, Japan). Integrated JEOL Analysis Station software was used for data collection and analysis. The coated sample itself was fixed onto the copper stage, ensuring the carbon-coated surface was in good contact with the holder. The analysis of cross-sections (mainly obtained by fragile cut) gives information about both non-homogeneous-in-layer and heterophase polymer structures, especially when combined with microprobe analysis. All analyses (spot and line) were performed under high vacuum conditions. The detector used for the EDX-DOT mapping spectrometer was an Oxford Inca X-act.

AFM Analysis.

All samples were coated on glass sheets. The surface morphologies of these polymer films were examined ex-situ by AFM (Bruker, Multimode 8) using sharp Si cantilevers with a radius of curvature of 5 nm working in contact mode. A large number of AFM images, each with a resolution of 512 × 512 pixels, were obtained over various parts of each sample. The value of Rq (the root mean square of the surface roughness height) was utilized to quantify the surface roughness of coatings. This was done to allow for better statistical averaging of values gained from AFM data. Peak Force QNM mode was used for the adhesion force analyses. Each sample was run 3 times.

Nanoindentation analysis

Nanoindentation experiments were performed using a Hysitron (Minneapolis, MN) TI 950 TriboIndenter equipped with a Berkovich probe at room temperature. Nano-DMA studies were typically performed on polymer films of P2 and P5 with areas of 1 × 1 cm^2 and thicknesses of 40 mm. DMA properties, such as the storage modulus (E′) and loss modulus (E″), were measured up to a frequency of 200 Hz, and the hardness was measured with a constant load of 100, 1000 μN; the system was calibrated using a fused silica standard with a series of indents to remove machine compliance effects from the experimental load depth traces. All measurements were repeated at least 5 times for each sample.

Flexibility test. The coating (160 μm thick) was made by casting the basic dispersion on PET. The PET film was bent into a "tube" form with a 1cm diameter. The force was then released, and the film was relaxed back to its original shape, completing the bending cycle. This bending cycle was performed 2000 times.

Abrasion test. The coating (160 μm thick) surface was crushed on a sandpaper (120 grit) with 1 kg loading on the glass slide. The slide was then dragged on the sandpaper for 20 cm before being restored to its original

position. This procedure was done several times to test the abrasion resistance of the coating and optical images are shown Figure S24.

Dynamic light scattering (DLS) and Zeta potential

DLS measurements were carried out on a Malvern Zetasizer Nano system equipped with a 633 nm He–Ne laser. 3 mL of the sample was used in a cuvette (PLASTIBRAND disposable cuvettes) and measured for 3 runs with a 10 s time interval. An average of at least three measurements was reported in the data. The zeta potential measurements Particle Metrix GMBH (made in Germany) measured in a very diluted solution of the polymer P5 in the THF/Ethanol (1:1). The diffusion coefficient calculated from the Stokes–Einstein expression $D = kT/6\pi\eta R$ (where kT representing the thermal energy at a temperature of T) the colloid particles of radius R in a liquid with a viscosity of η.

Table S1. Material compositions used for the synthesis of the polymeric material

Polymer	Material	PVA g (mmol)	TA g (mmol)	TEOS g (mmol)	Pentanal g (mmol)
	oligosiloxanes	-	-	0.500 g	-
P1	PVA-oligosiloxanes	0.44 (10.0)	-	0.313 (1.5)	-
P2	**PVA-TA-oligosiloxanes**	**0.44 (10.0)**	**0.125 (0.07)**	**0.313 (1.5)**	**-**
P3	PVA-VD	0.44 (10.0)	-	-	0.5 (5.8)
P4	(PVA-oligosiloxanes)-VD	0.44 (10.0)	-	0.313 (1.5)	0.5 (5.8)
P5	**(PVA-TA-oligosiloxanes)-VD**	**0.44 (10.0)**	**0.125 (0.07)**	**0.313 (1.5)**	**0.5 (5.8)**

Synthesis:

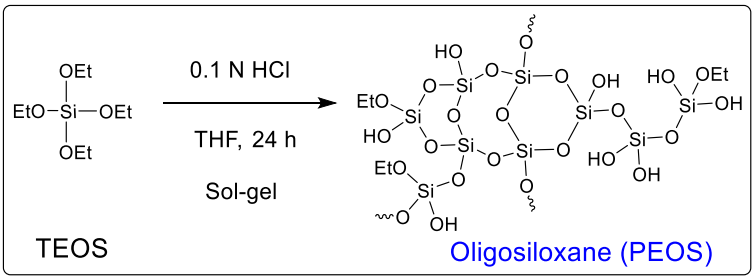

Scheme S1. Synthesis of oligosiloxanes by sol-gel process

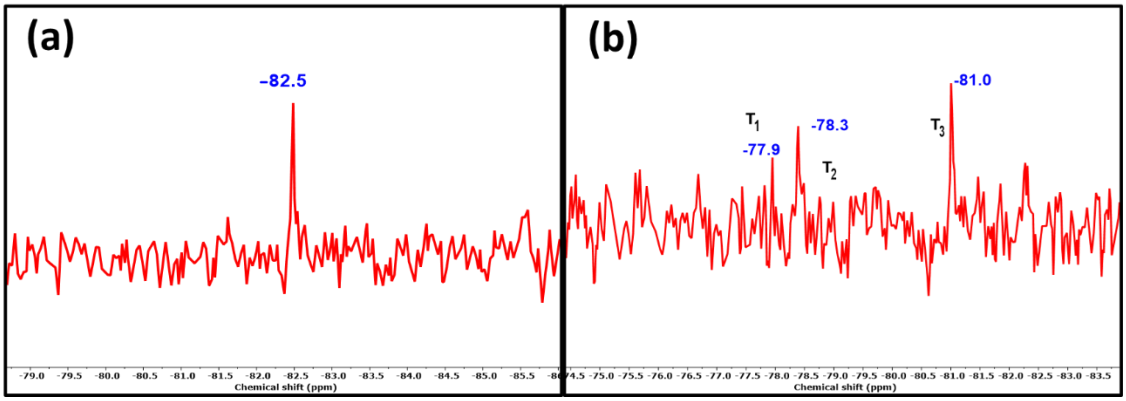

Figure S1. (a) ^{29}Si NMR of TEOS, **(b)** ^{29}Si NMR of oligosiloxanes and P2.

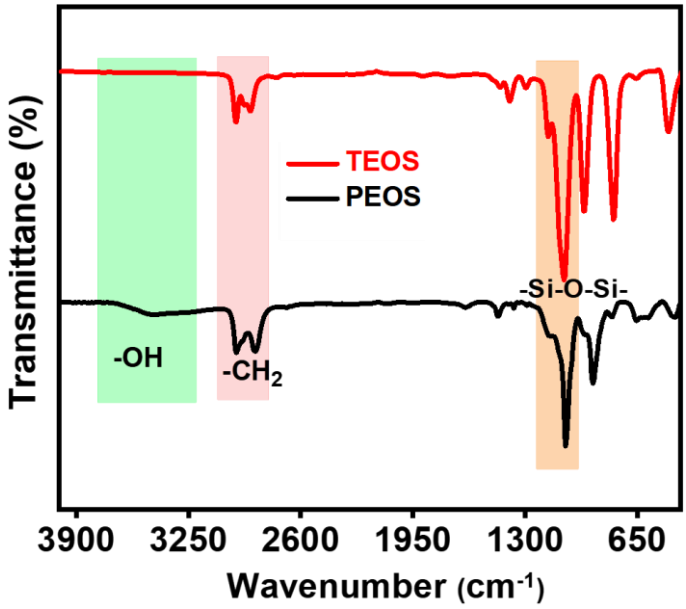

Figure S2. FT-IR spectra of oligosiloxanes [poly(tetraethyl orthosilicate), **PEOS]**

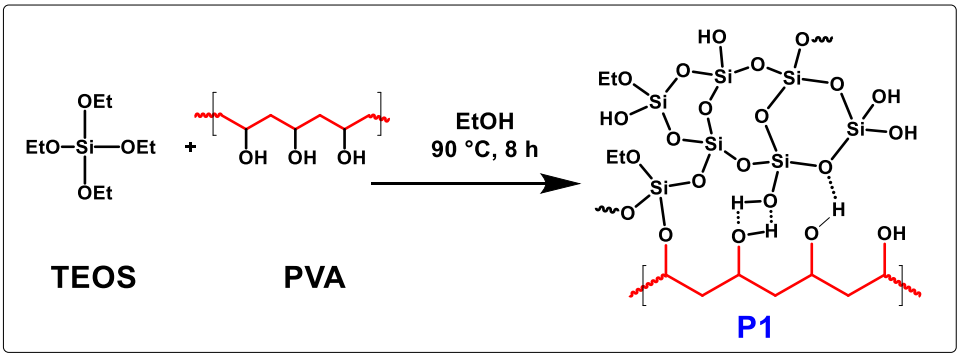

Scheme S2. Synthesis of PVA-oligosiloxane, **P1**

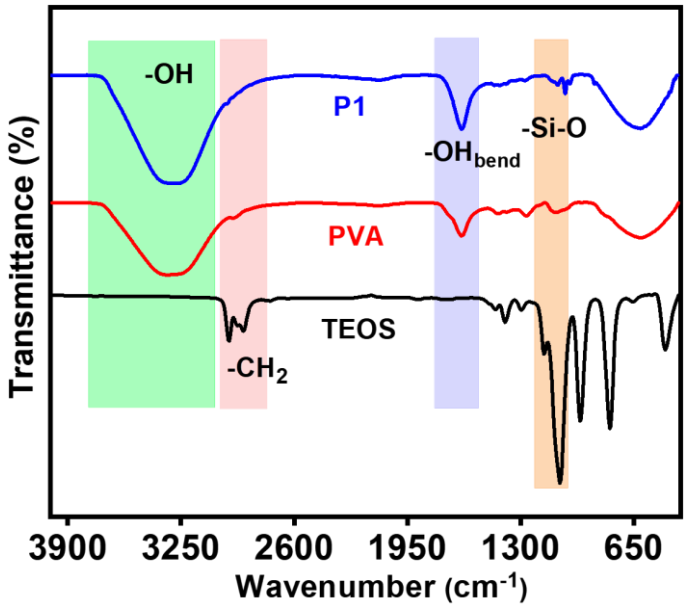

Figure S3. FT-IR analysis of the PVA-oligosiloxane, **P1** compared with PVA and TEOS

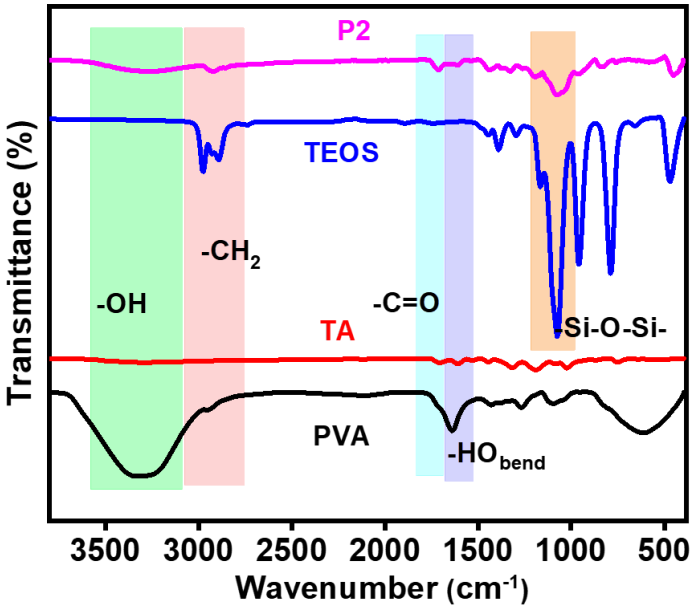

Figure S4. FT-IR analysis of the poly(vinyl alcohol-tannic acid-oligosiloxane), PVA-TA-oligosiloxanes, **P2** compared with PVA, TA and TEOS

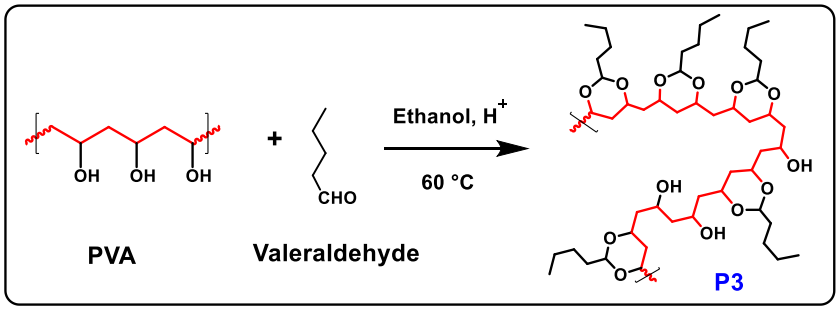

Scheme S3. Synthesis of poly(vinylacetal), PVA-VD**, P3**

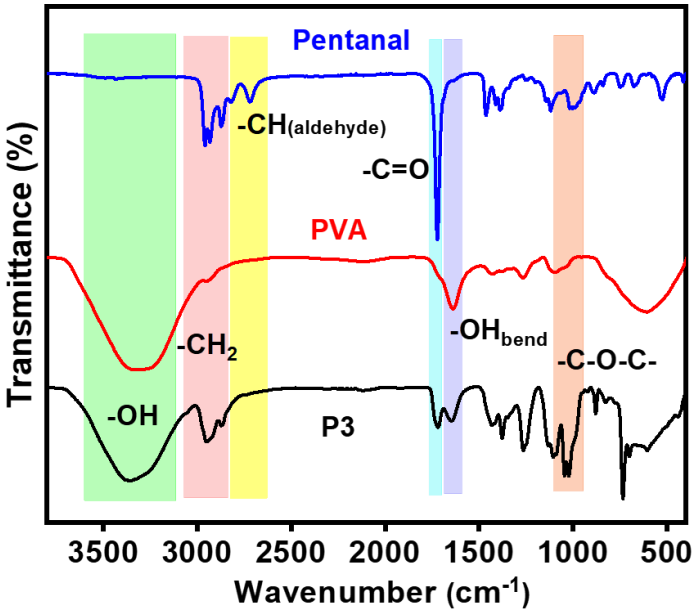

Figure S5. FT-IR analysis of PVA-VD (**P3**) compared with PVA and pentanal.

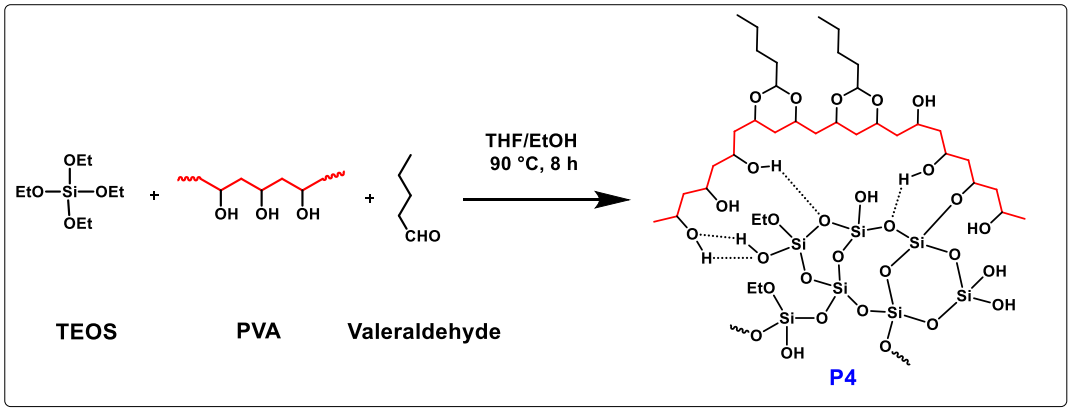

Scheme S4. Synthesis of (PVA-oligosiloxanes)-VD, **P4**

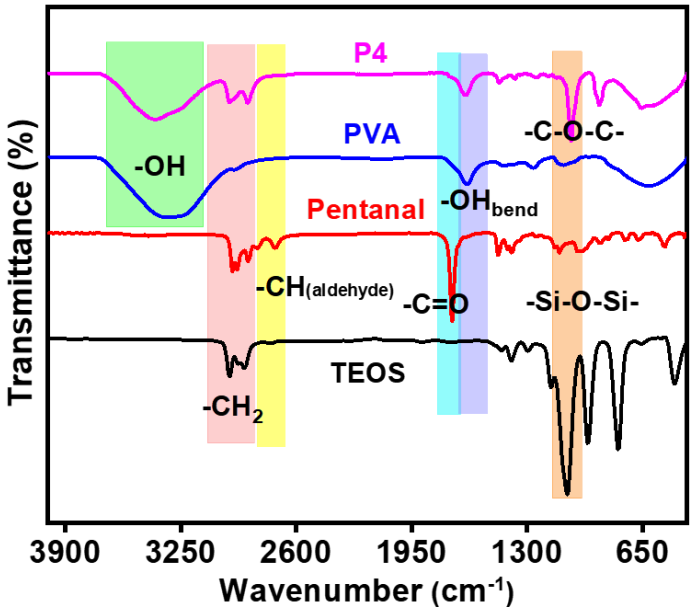

Figure S6. FT-IR analysis of the (PVA-oligosiloxanes)-VD, **P4,** compared with TEOS, pentanal and PVA

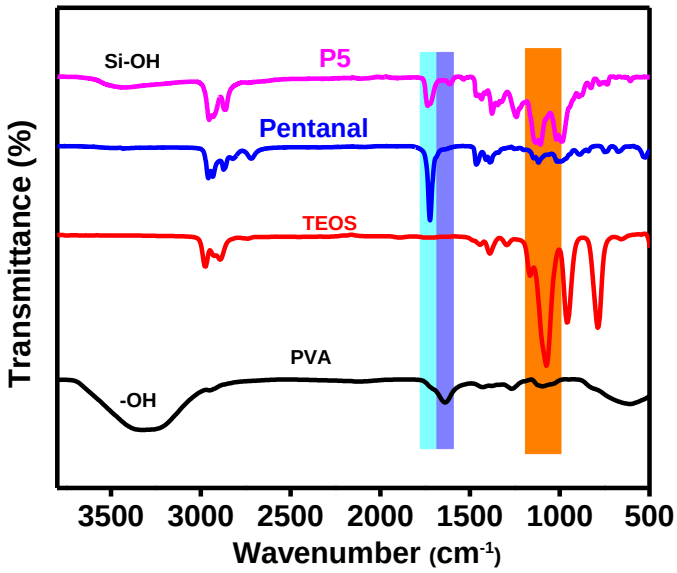

Figure S7. FT-IR of (PVA-TA-oligosiloxanes)-VD, **P5** compared with PVA, TEOS, and valeraldehyde.

Dynamic light scattering (DLS):

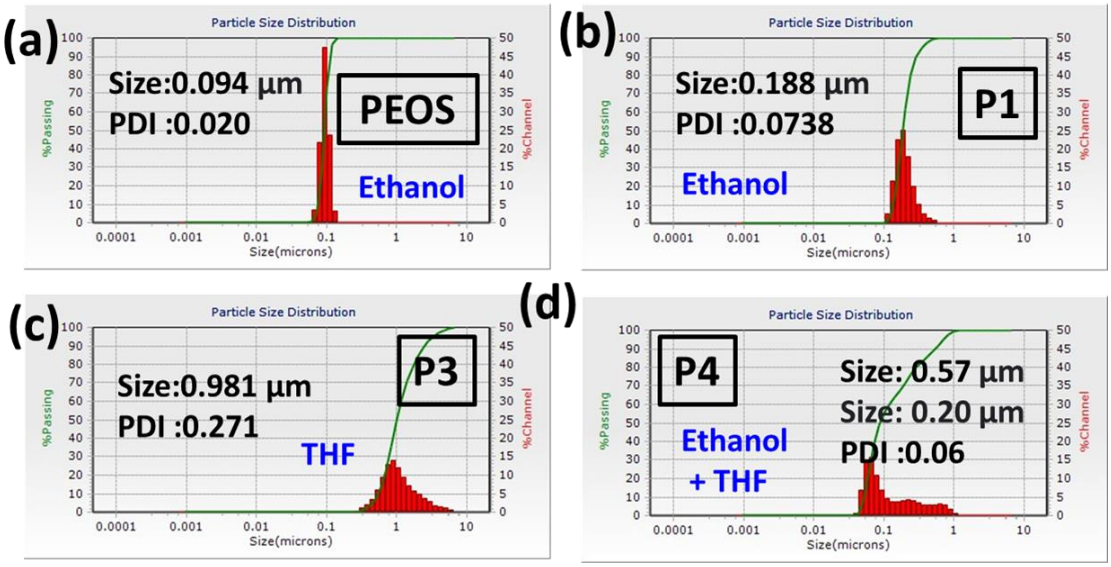

Figure S8. Particles distribution of the polymers oligosiloxanes (**PEOS), P1**, **P3** and **P4**.

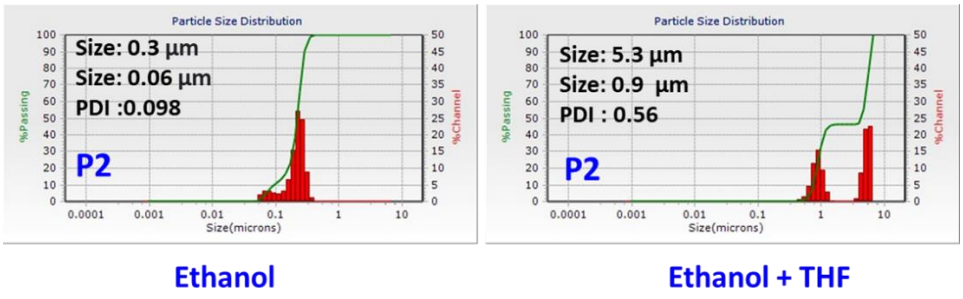

Figure S9. Particle size distribution from DLS of **P2** in ethanol and THF+ethanol.

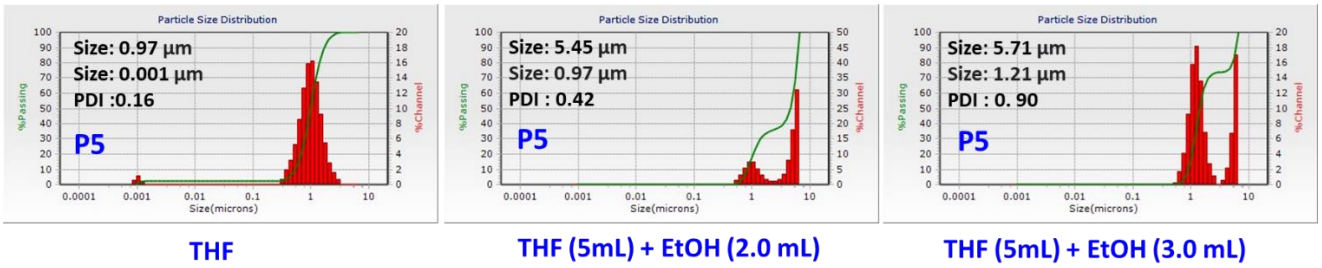

Figure S10. Particle size distribution from DLS of **P5** in THF + ethanol

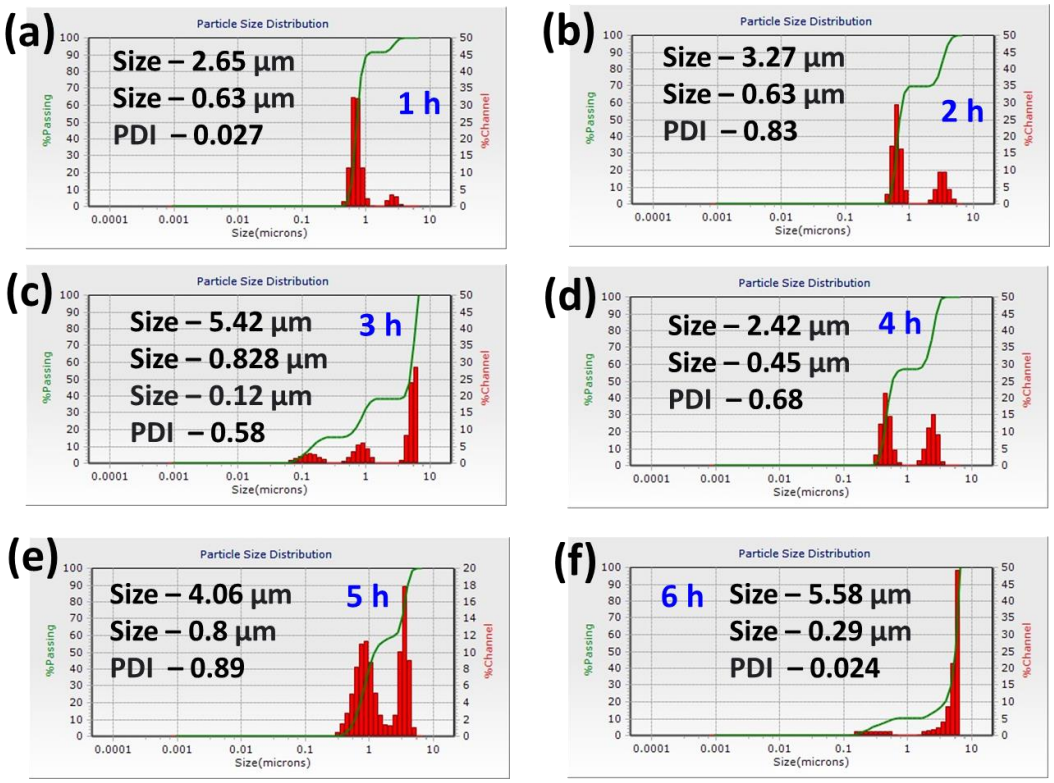

Figure S11. Particle size distribution from DLS of **P5** by varying the concentration of VD throughout time**.**

Table S2. Calculated diffusion coefficient of **P5** at the different concentration if THF/Ethanol

THF/Ethanol (mL)	**R_h (µm)** (Large particles)	**R_h (µm)** (Small particles)	**Diffusion coefficient ($D_{(Large)}/D_{(Small)}$)**
1.0/ 0.0	0.97	0.001	0.14/-
1.0/0.50	5.45	0.97	0.14/0.025
1.0/0.55	5.71	1.21	0.12/0.025

Figure S12. Oligosiloxanes coated on the glass plate

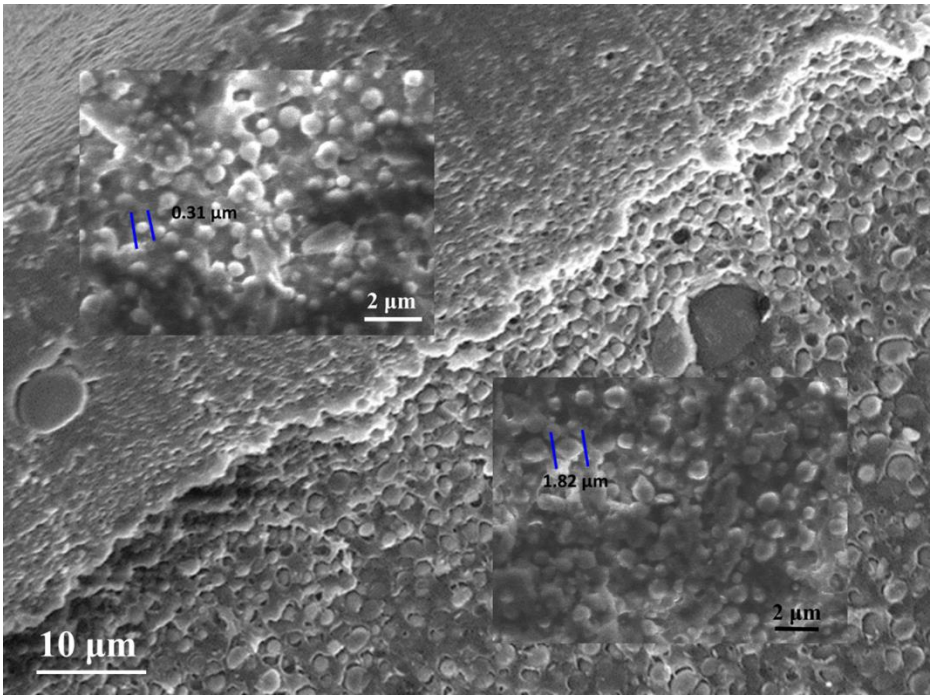

Figure S13. The cross-section morphology of **P5** coated on **glass** substrate, segregation of small and large particles between the two layers having diameters ~0.31 µm and 1.82 µm, respectively.

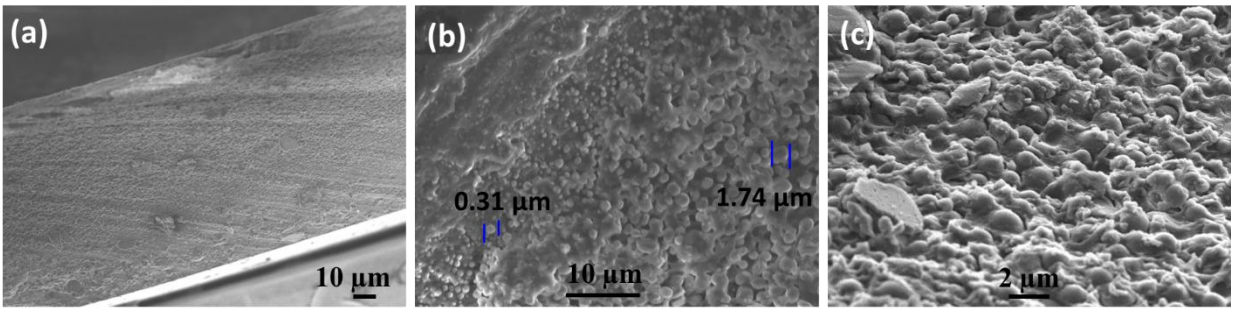

Figure S14. (a) cross-section morphology of **P5** coated on **Teflon**; (b) and (c) zoomed part.

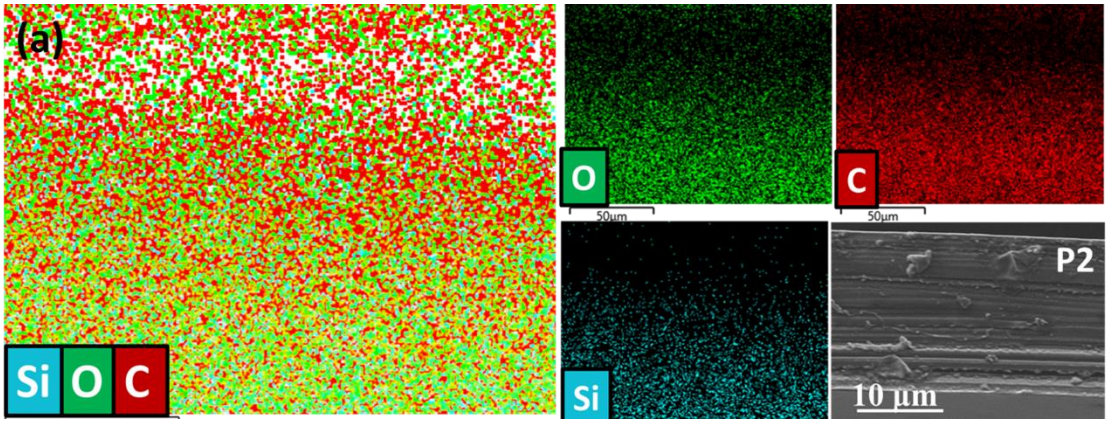

Figure S15. (a) Cross-section morphology and EDS-DOT mapping of the area of **P2** coated on the glass.

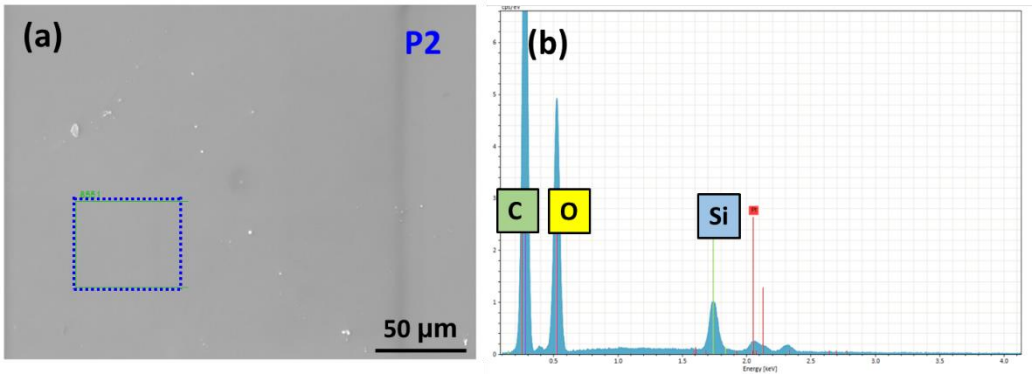

(c)

Element	Mass Norm. (%)	Atom (%)
Carbon	53.99	62.99
Oxygen	40.07	35.10
Silicon	3.44	1.71
Platinum	2.48	0.17

Figure S16. (a) Surface morphology and (b) elemental distribution (C, O, and Si) of the surface of **P2** coated on the glass surface. (Platinum appeared from thin film coating to eliminate charging).

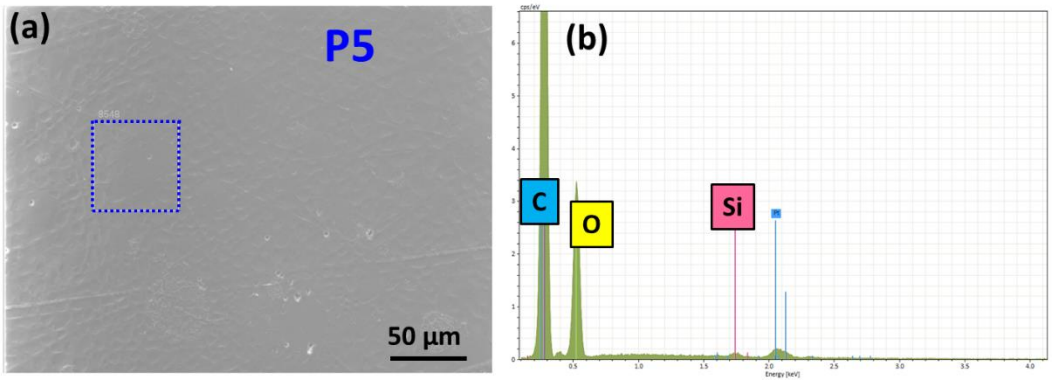

(c)

Element	Mass Norm. (%)	Atom (%)
Carbon	65.67	73.11
Oxygen	31.75	26.54
Silicon	0.40	0.195
Platinum	2.16	0.14

Figure S17. (a) Surface morphology of the polymer **P5**; (b) Elemental distribution (C, O, and Si) on the surface of **P5**, coated on the glass surface. (Platinum appeared from thin film coating to eliminate charging).

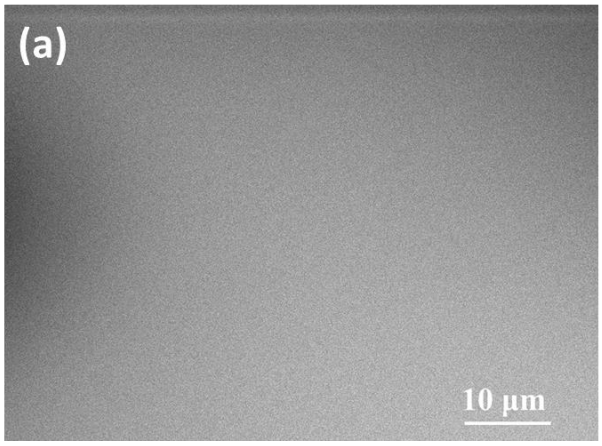

Figure S18. (a) Surface morphology of the polymer **P5,** coated on the Teflon substrate**.**

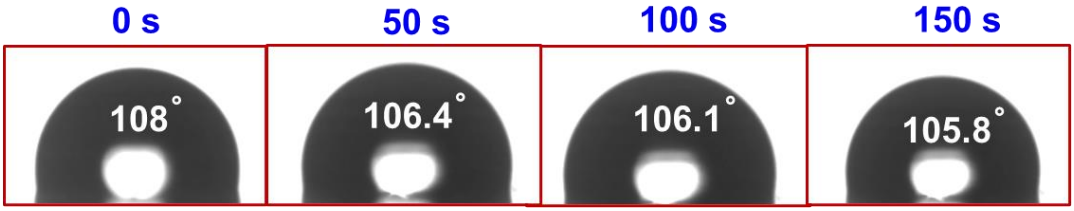

Figure S19. Dynamic water contact over the time of **P5** coated on the glass.

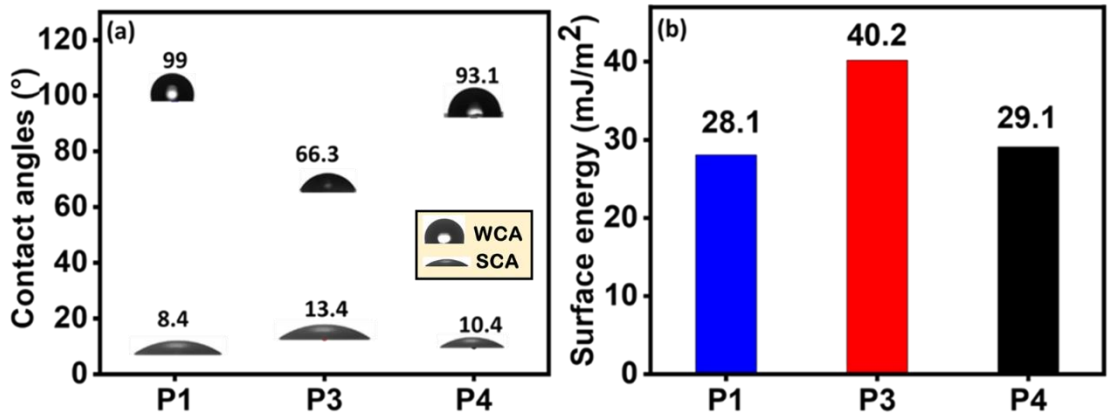

Figure S20. Water contact angles and solvent contact angles of **P1, P3** and **P4** and corresponding surface energy.

Water stability test:

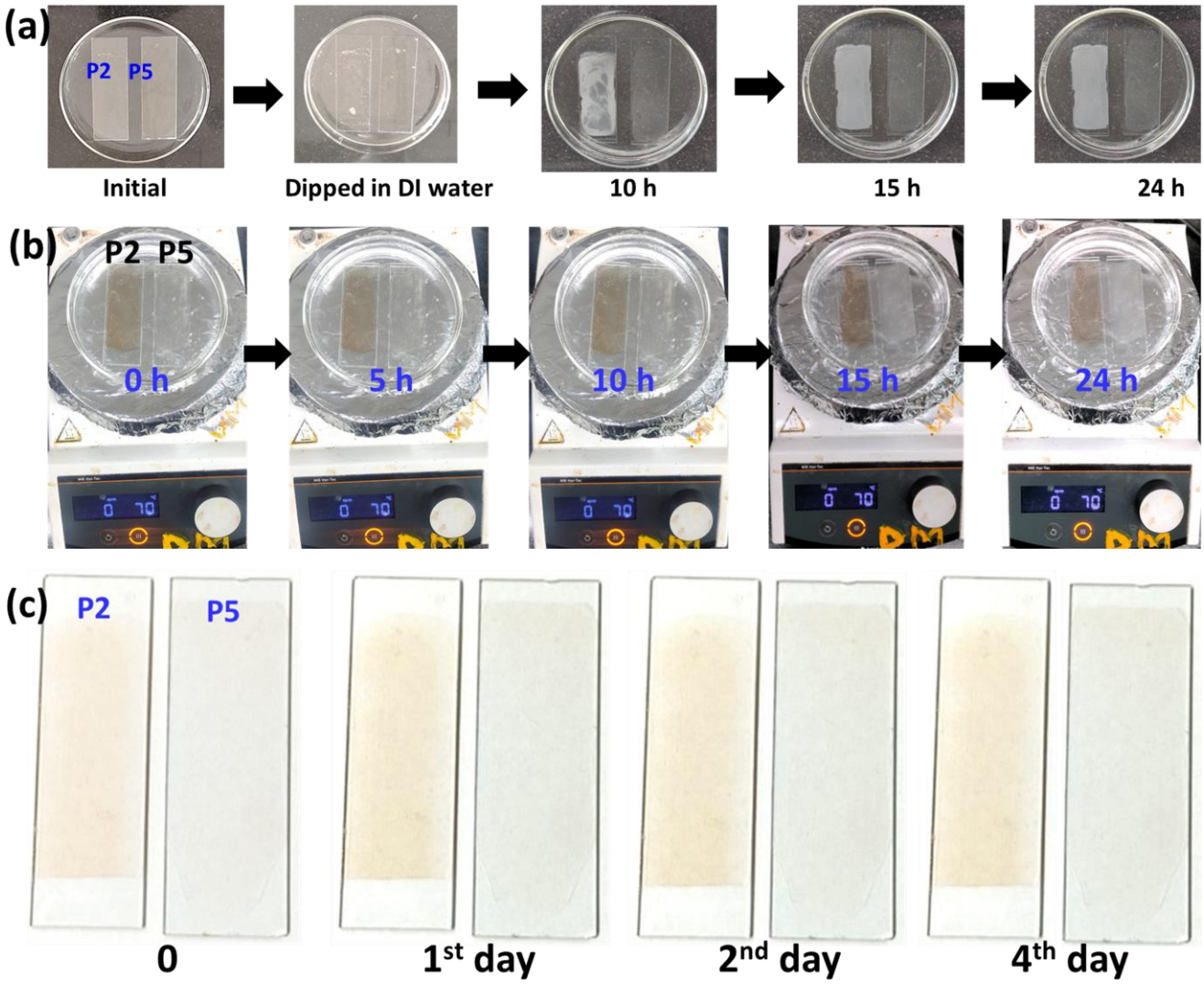

Figure S21. (a) Underwater stability of the P2 and P5 at room temperature, (b) in hot water at 70 °C; (c) P2 and P5 coated glass slide exposure to direct sunlight (time counted everyday 11 h of sunlight).

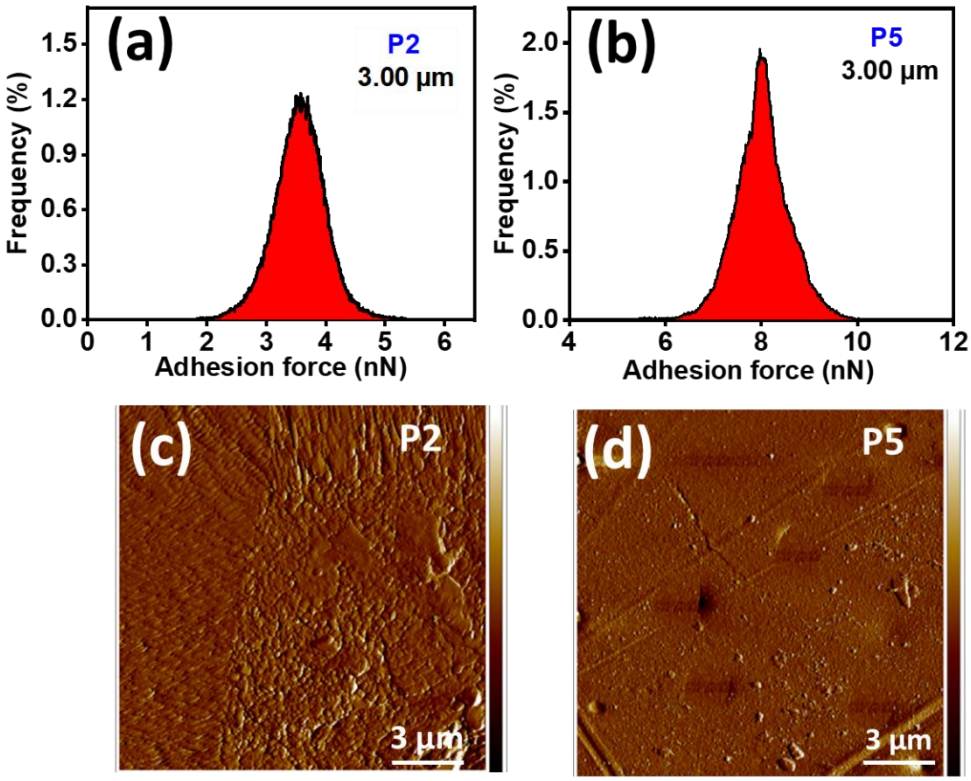

Figure S22. (a) and (b) Adhesion forces, and (c) and (d) corresponding morphology of **P2** and **P5** coated on glass on the area of 3×3 μm^2.

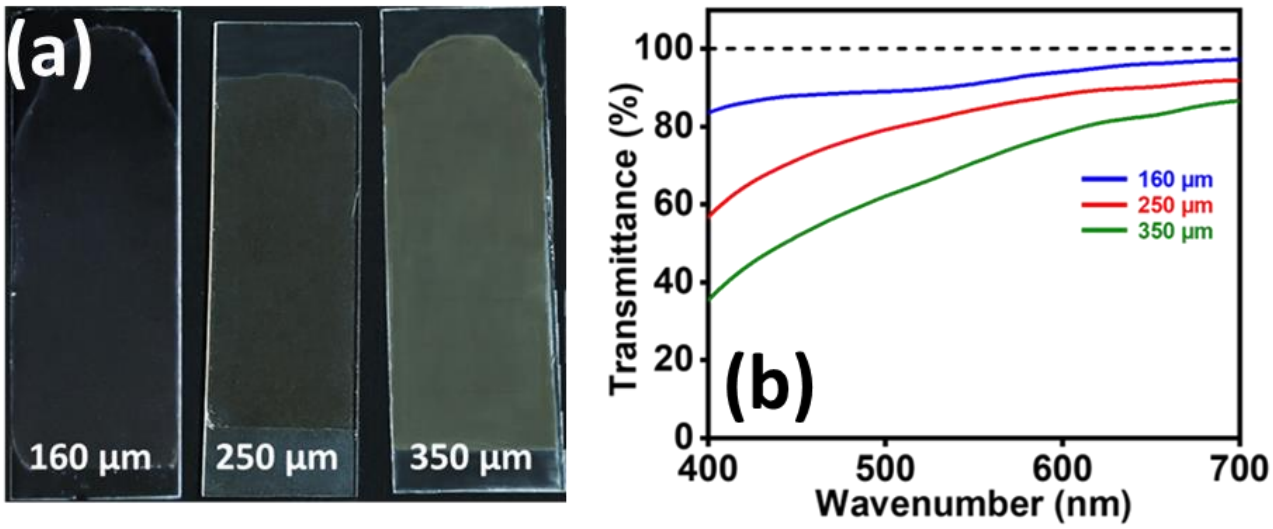

Figure S23. (a) Photograph of the glass coated films of different thickness, and (b) corresponding transmittance.

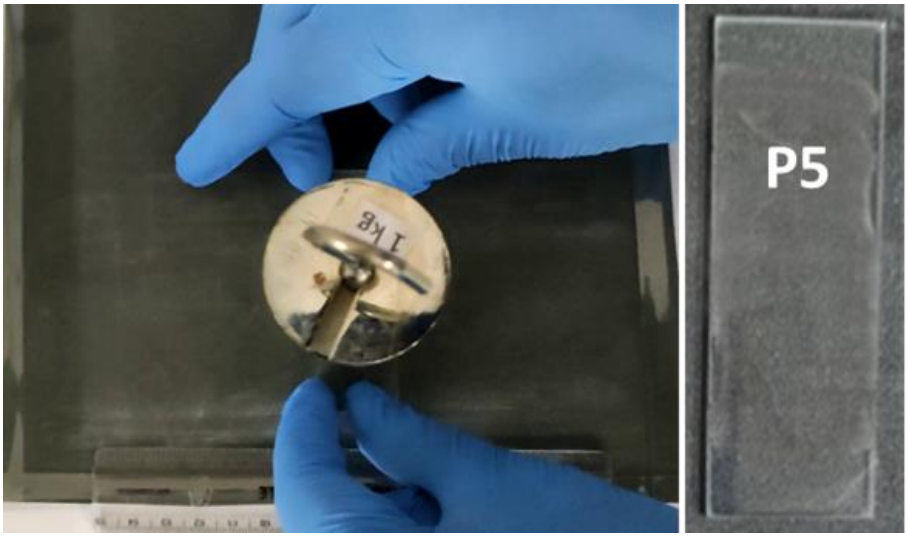

Figure S24. (d) Abrasion test of P2 and P5 coating on glass over sandpaper of 120 grit.

Abrasion test. P5 coating (160 μm thick) surface was crushed on a sandpaper (120 grit) with 1 Kg loading on the glass slide. The slide was then dragged on the sandpaper for 20 cm before being restored to its original position. This procedure was done several times to test the abrasion resistance of the coating and optical images are shown Figure S24.

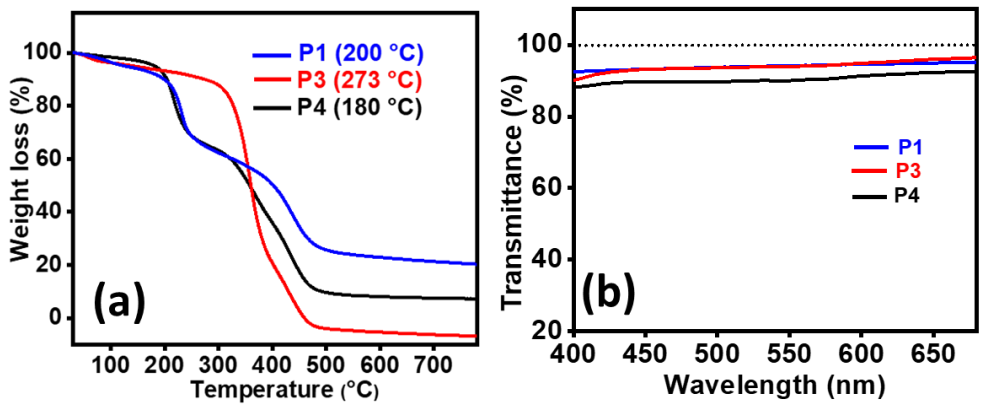

Figure S25. (a) TGA graphs of **P1, P2** and **P3** (T_{onset} in parenthesis); (b) transmittance of **P1**, **P2** and **P3** compared with glass substrate.

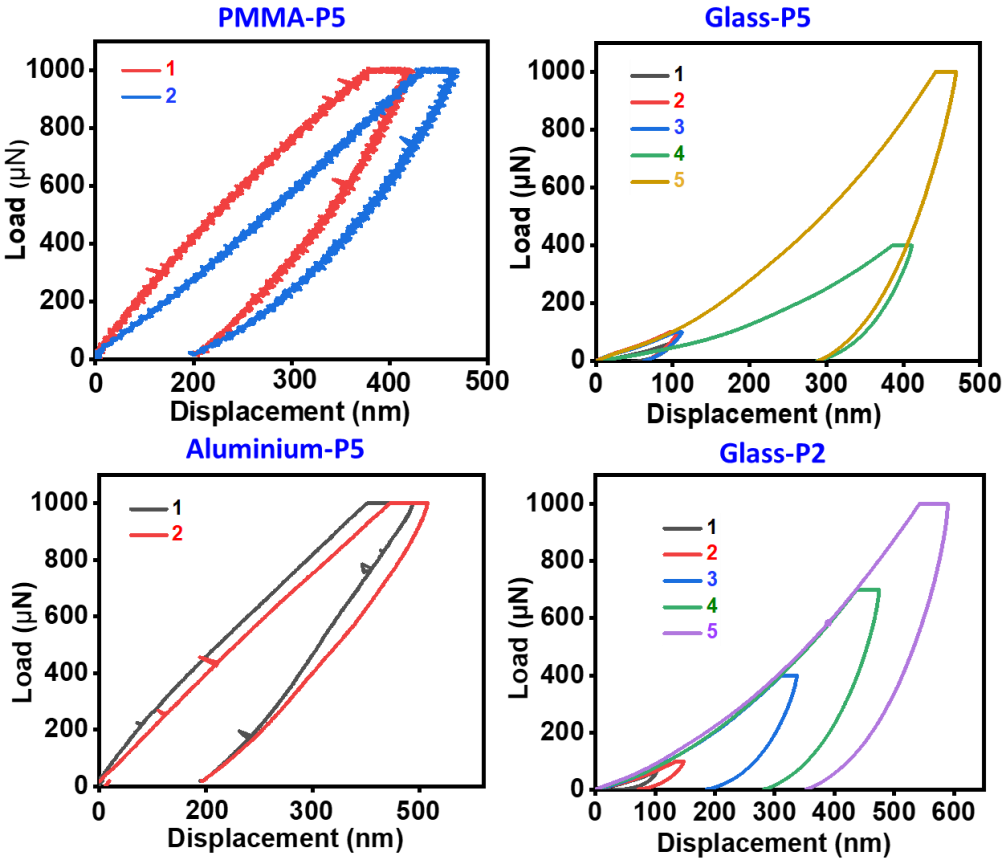

Figure S26. Nanoindentation load-displacement curves of **P2** and **P5** coating on different substrates.

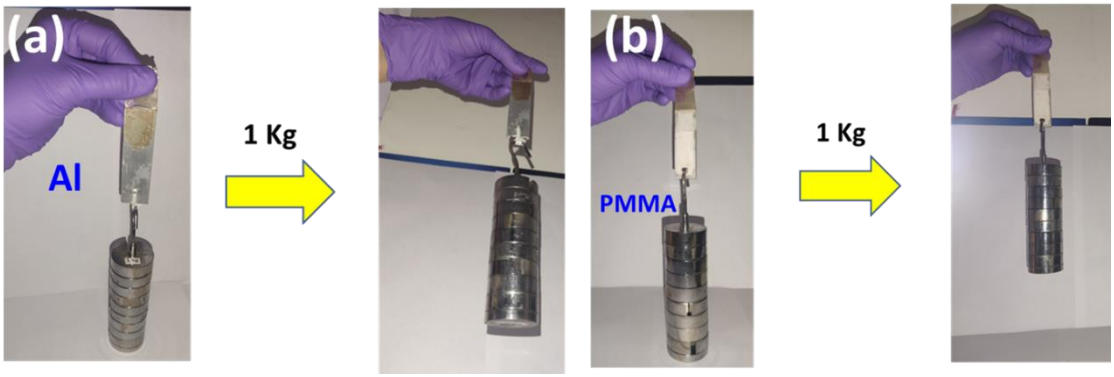

Figure S27. The hanging of the 1 kg load on the Aluminium and PMMA sheet attached with a **P5**

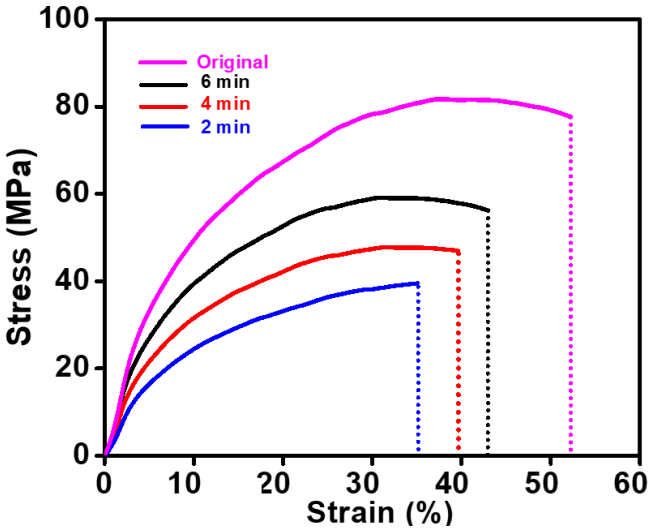

Figure S28. Time dependent self-healing performance of P2 sheet.

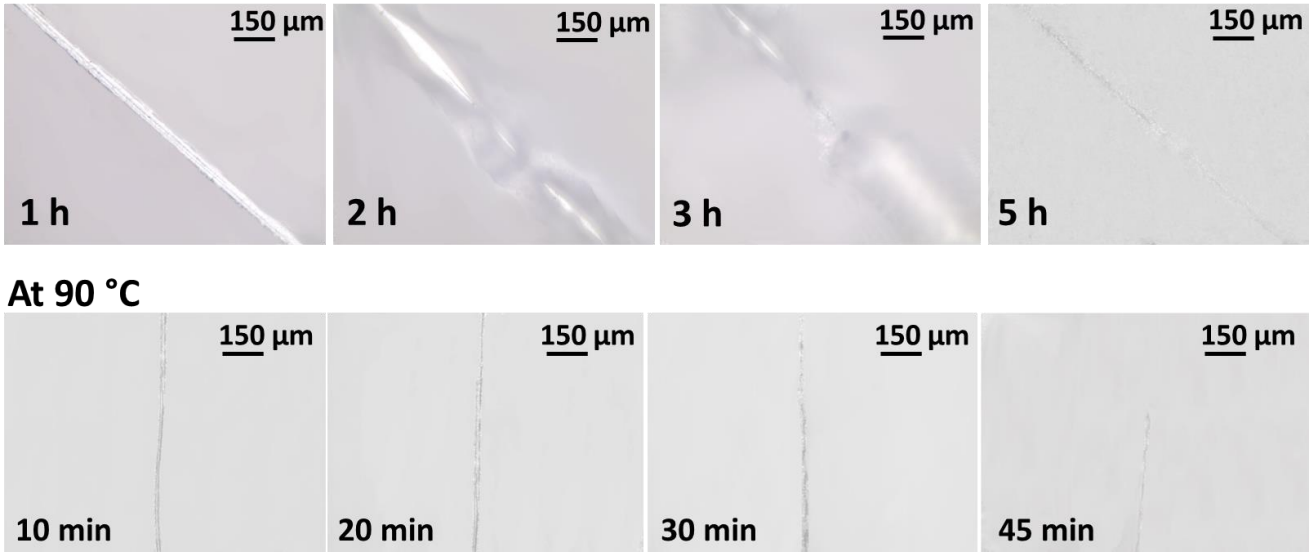

Figure S29. (a) Optical images of healing with time at 45 °C; (b) at 90 °C.

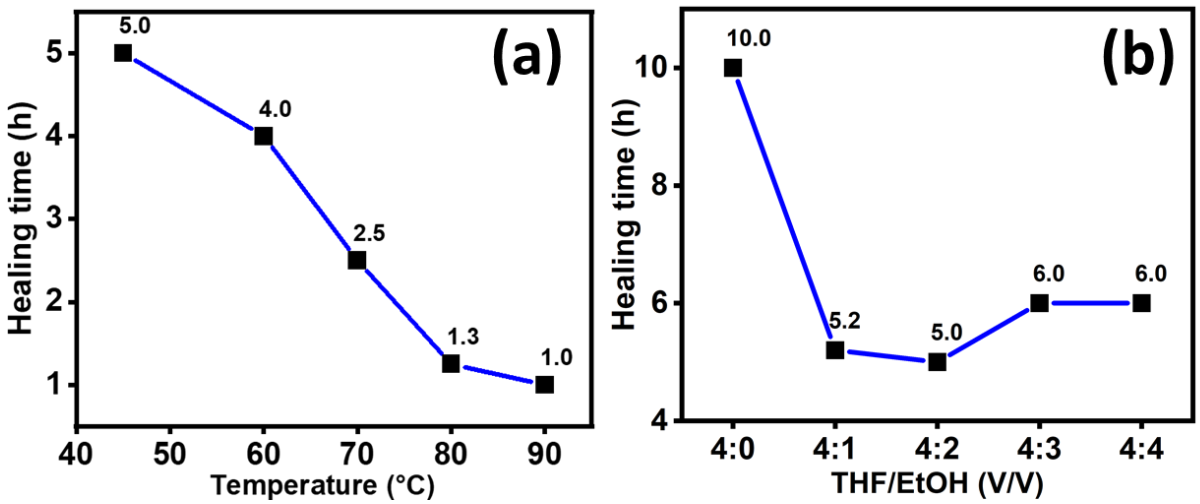

Figure S30. Healing performance (a) with variation of the temperature; (b) with respect to the variation of volume fraction variation of small and big particles ($V\phi s : V\phi_L$) with different THF/ethanol solvent ratios.

Supplementary Movies.

Movie M1. Video showing the coating stability of **P5** coated on glass at 150 °C. The experiment has done for over 5 minutes.

Movie M2. Video showing the low-temperature (liquid nitrogen) stability at the different substrates (glass, aluminium) of **P5** coated on glass.

Movie M3. Video showing the anti-icing properties of **P5** (compared with the bare glass) at -80 °C for 24 h inside -80 deep freezer.

Table S3. Comparison of Adhesion strength and Hardness of P5 with reported literature on siloxane-based coatings.

	Substrate	Adhesion strength (MPa)	Hardness (GPa)	Durability	Wettability (WCA)	Advantages	References
1	**Glass**	**4.65**	**0.520**	Flexibility, abrasion resistance, good hardness, wear resistance, good adhesion against heat (150 °C) and liquid N2 stability and water, solar radiation resistance	108°	Self-stratified, Anti-icing, and self-healing coating	This work
2	**Aluminium**	**12.63**	**1.0**				This work
3	Glass	3.61	0.224	Flexibility, abrasion resistance, good pencil hardness, wear resistance	83.4°	Anti-fouling coating	*Adv. Funct. Mater.* 2021, **31**, 2011145
4	Glass	2.62	0.131	Flexibility, abrasion resistance, good pencil hardness, wear resistance	99.8± 0.7°	Anti-fouling and anti-smudge coating	*Adv. Sci.* 2022, 2200268
5	Glass	2.9	-	Highly elastic	105-110°	Self-healing, Anti-fouling	*J. Mater. Chem. B*, 2021, **9**, 1384-1394
6	Glass Fiber	<1.0	-	Not mentioned	105-110°	Self-repairing, Anti-biofouling	*J. Mater. Chem. A*, 2017, **5**, 15855-15861
7	Glass	0.069.4	-	Not mentioned	-	Underwater adhesive	*ACS Appl. Mater. Interfaces* 2020, **12**, 20933–20941
8	Glass	1.8	0.570	Flexibility at 100 cycles on PET film	117°	fouling release and resistance abilities	*J. Mater. Chem. A*, 2020, **8**, 380–387
9	Glass	-	1.4	Flexibility, abrasion resistance, good pencil hardness, wear resistance	112°	Rollable Omniphobic coating	*ACS Appl. Mater. Interfaces* 2022, **14**, 35138–35147
10	Glass	-	0.83	Flexibility, abrasion resistance, good pencil hardness, wear resistance, UV resistance and high heat resistance	83°	Self-healing and Multifunctional Nanocomposite coatings	*J. Am. Chem. Soc.* 2022, **144**, 436–445